Chapter 12
Applications and Working Mechanism of Fe_2O_3 Nanoparticle and Its Composite for Wastewater Treatment

Manoj Kumar Sahu, Hari Sankar Mohanty, Raj Kishore Patel, and Sudarshan Khudwakar

Abstract The impacts of various added substances on the morphology and related photocatalytic properties of different hematite (α-Fe_2O_3) nanostructures were examined. α-Fe_2O_3 croissant-like designs and finished microspheres were framed by aqueous treatment at 120 °C for 6 h within the sight of NaCl, Na_2SO_4, and $Na_2C_2O_4$ as added substances, separately. After heat treatment in air, the photocatalytic movement of the α-Fe_2O_3 powder was surveyed by degrading methyl orange (MO) under UV light with hydrogen peroxide (H_2O_2) as an activator. The α-Fe_2O_3 progressive designs displayed the best photocatalytic activity with a 76.5% evacuation or degradation of dye molecules. This is credited to the high surface region of the iron oxide like morphology, which gives more dynamic locales for the degradation of dyes. The activation energy has also been well compared to the kinetic and isotherm models in the review, which shows that degradation of dyes on the outer layer of iron oxide is much more effective.

Keywords Iron oxide · Nanoparticles · Degradation · Dyes · Wastewater

M. K. Sahu (✉)
Department of Chemistry, GIET University, Gunupur, Odisha 765022, India
e-mail: manojsahu.pdm@gmail.com

H. S. Mohanty
Department of Physics, GIET University, Gunupur, Odisha 765022, India

R. K. Patel
Department of Chemistry, National Institute of Technology, Rourkela 769008, India

S. Khudwakar
Department of Civil and Environmental Engineering, California State University, 800 N. State College Blvd., Fullerton, CA 92831, USA

H. Sahoo and J. K. Sahoo (eds.), *Iron Oxide-Based Nanocomposites and Nanoenzymes*, Nanostructure Science and Technology, https://doi.org/10.1007/978-3-031-44599-6_12

12.1 Introduction

Water is the most precious resource and is crucial for all living creatures in its pure state on earth. It plays a key role in the world economy. An exclusively broad spectrum of hazardous contaminants is released into the watercourse due to rapid urbanization, industrialization, population growth, and long-term droughts, which has grown to be a serious issue worldwide [1–4]. So far, industries have generated a huge amount of miscellaneous carcinogenic contents, and the disposal of these untreated contaminants has been observed to be the main source of water pollution [5, 6]. This may lead to major social evils such as drinking water deficits [7], water evaporation [8], and surface water contamination [7]. The most important factors contributing to this global water pollution are industrial sewage containing hazardous dyes and heavy metals, along with some poisonous chemicals. In fact, these untreated industries discharged the contaminants that contaminate surface water as well as groundwater by spreading their toxicity and causing severe protozoan infections, fungal attacks, and other deadly diseases in aquatic organisms [9–11]. These pollutants, which have tempted increasing concerns about wastewater, can cause adverse ecological problems for wildlife and the environment, such as health effects and mutagenic effects in human beings, aquatic beings, and other living beings [12]. Moreover, the release of these miscellaneous dyes as well as a number of toxic natural contaminants in soils and aqueous environments has made the global water source's condition of inferior quality [13].

Commonly, dyes are classified into two major types such as: herbal/natural and synthetic/artificial dyes. Natural dyes are derived from plant resources such as leaves, roots, wood, berries, fungi, bark, and lichens, whereas synthetic dyes are produced from chemicals, earth minerals, and petroleum derivatives [3, 4]. Artificial dyes are considerably used in sports as well as in paper; in printing, they are used as colorants, and they are also used in the beauty and leather industries too [14]. It has been previously affirmed that dyes were comprehensively used in textile industries (~200,000 tons/year), and without a precise remediation method, they were tended to release into the sewage [2, 15].

In general, dyes possess a very complicated shape with a high molecular weight, are water-soluble, degradation-resistant, potentially carcinogenic as well as mutagenic, and also have the tendency to inhibit sunlight penetration and reduce photosynthetic reactions [6]. The water pollutants may be labeled into numerous principal types, which include natural and inorganic contaminants, vitamins, agricultural waste, pathogens, suspended solids, radioactive wastes, and thermal pollution as well [16].

Generally, there have been various treatment methods implemented to eliminate hazardous organic contaminants from aqueous solutions over the past decades [17]. Several chemical, physico-chemical, and biological techniques, such as membrane separation [18], flocculation [19], adsorption [20], coagulation [21], fungal decolonization [22], degradation [23–26], and ultra-chemical treatments [27], have been widely implemented for the successful removal of dyes from wastewater. Among

those methods, chemical degradation by the advanced oxidation process (AOP) has been proven to be the most efficient one for the resolution of these hazardous chemicals due to their refractory and persistent structure [28]. This process has also been demonstrated to be much more efficient, non-toxic, cost-effective, easy-handling, energy-saving, and eco-friendly in nature.

In the present scenario, nanotechnology has materialized as a cutting-edge technology and a state-of-the-art with broad applications in every field of life. At present, scientists and researchers are putting more focus on the fabrication of nanocomposite, and various techniques are also being implemented for this purpose [29]. Physical methods and chemical techniques are conventionally applied to prepare these nanosheets. Furthermore, magnetic nanocomposites consist of a significant group of inorganic materials and propose a number of applications in research fields by virtue of their unique and distinctive properties [30].

Magnetic nanostructures hold the capability to remove these finely shaped nanoparticles of toxic dyes, heavy metals, and colloids, which cause a very problematic situation when they are supposed to be removed by those pre-conventional techniques. Among those several magnetic nanocomposites, iron oxide has been considered to be the most efficient as well as convenient for the adsorption technique due to its very small size and ferromagnetic nature [31]. They have the potential to remove several heavy metal ions, such as lead, cadmium, copper, or chromium, as well as dyes and pesticides, simultaneously from wastewater [32]. In current times, the application of magnetic nanoadsorbents for the decontamination process has become very efficient and has received considerable demand and attention due to their easy separation ability [33–38]. The iron oxide possesses many kinds of phases, such as FeOOH, FeO, Fe_4O_5, Fe_3O_4, Fe_4O_3, $Fe(OH)_3$, polymorphs of Fe_2O_3 (α-Fe_2O_3, and γ-Fe_2O_3), and so on. Among these, maghemite (γ-Fe_2O_3), hematite (α-Fe_2O_3), and magnetite (Fe_3O_4) are of greater interest for their drinking water treatment, electrical, magnetic properties, optical properties, ferrofluid technology, magneto caloric refrigerant, gas sensing, etc. [39–42]. This compound has a lot of influence and impact on the remediation of water, such as fast and easy production, rapid uptake, high adsorptive capacity, easy separation, etc.

Over the last few years, the elimination of different organic dyes has grown to be a global concern considering their carcinogenic effects on the environment. Approximately 70–80% of total illnesses in women and children in developing countries are initiated by different water contaminants, according to WHO and UNICEF reports from 2000. The several toxic things caused by dyes are shown in Fig. 12.1. Thus, in this session, different applications of Fe_2O_3 in the removal of organic dyes and pesticides are discussed.

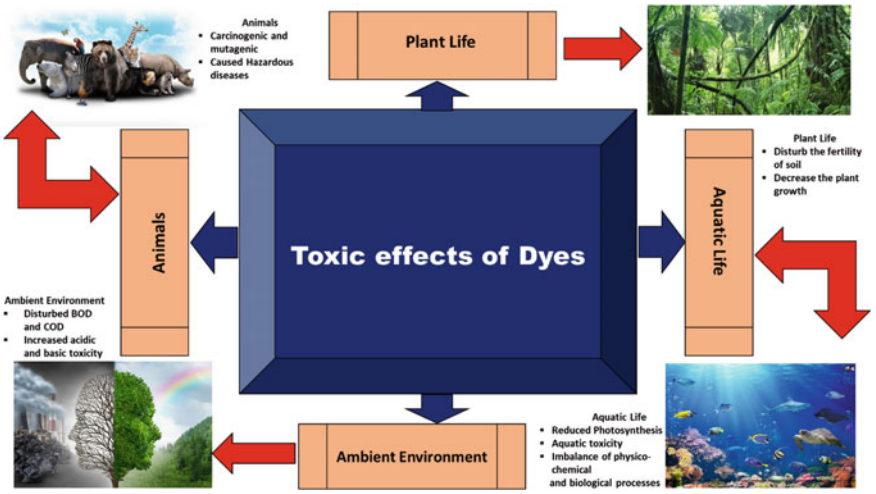

Fig. 12.1 Toxic things caused by dyes on environment and living beings

12.2 Removal of Organic Dyes

A dye is a substance that imparts color through physical or chemical binding. The chromophoric units present in the dye develop a color to which auxochromes are attached. Dyes are used in various applications in our day-to-day lives that release toxic organic and inorganic chemicals from industries wastewater, resulting in harmful effects on the environment. Therefore, it is essential to protect the environment from the toxic effluents released into the water body by treating them through different physical, chemical, and biological treatments. In the following sections, the adsorptive and photocatalytic removal of dyes using various classes of adsorbents and catalysts and their adsorptive and photocatalytic mechanisms are presented.

Guo et al. synthesized a heterogeneous Fenton catalyst i.e., α-Fe_2O_3/$Cu_2O(SO_4)$, which was highly efficient as well as a novel reagent for the removal of organic dye in the field of advanced oxidation processes (AOPs). It had become a widespread investigation which resulted in the formation of $Cu_2O(SO_4)$-Fe_9 [43] composite showing brilliant catalytic removal efficiency for the degradation of orange II. Considering its effectiveness, it showed the rate of removal of about 98.9% at 50 mg/L Orange II in 100 ml (under the condition of 0.3 g/L $Cu_2O(SO_4)$-Fe_9 catalyst, 3 mm H_2O_2, and pH = 3.5). In this concern, PL spectra were used to measure the dissociation efficiency of photon-generated carriers. The intensity of this PL spectra indicated that the $Cu_2O(SO_4)$-Fe_9 nanocomposite excited the dissociation of carriers by showing the peaks as $Cu_2O(SO_4) > \alpha$-$Fe_2O_3 > Cu_2O(SO_4)$-Fe_9. Again a number of scavengers like 1,4-benzoquinone, isopropanol, CCl_4, and CH_3OH were added to the photo-fenton system to adsorb the superoxide, hydroxyl radicals, electrons, and holes respectively. When the rate of degradation of Orange II was compared without and along with the scavengers, it was found that when isopropanol (10 mM) was added to the system,

the degradation efficiency of Orange II was decreased to 21.4% from 98.9% within 15 min. Based on this decreasing efficiency, the catalytic mechanism was analyzed as shown below.

$$\mathrm{Fe^{3+}_{surf} - OH + H_2O_2 \rightarrow (H_2O_2)_S} \tag{12.1}$$

$$\mathrm{(H_2O_2)_S \leftrightarrow Fe^{2+}_{surf} - \cdot O_2H + H_2O} \tag{12.2}$$

$$\mathrm{Fe^{2+}_{surf} - \cdot O_2H \leftrightarrow Fe^{2+}_{surf} - \cdot O_2H} \tag{12.3}$$

$$\mathrm{(H_2O_2)_S \leftrightarrow Fe^{2+}_{surf} - \cdot O_2H + H_2O} \tag{12.4}$$

$$\mathrm{Fe^{2+}_{surf} + H_2O_2 \rightarrow Fe^{3+}_{surf} - OH + \cdot OH} \tag{12.5}$$

$$\mathrm{Fe^{2+}_{surf} - OH + \cdot O_2H \rightarrow Fe^{2+}_{surf} + H_2O + O_2} \tag{12.6}$$

$$\mathrm{Fe^{3+} + H_2O_2 \rightarrow Fe^{2+} + \cdot O_2^- + 2H^+} \tag{12.7}$$

$$\mathrm{Fe^{2+} + H_2O_2 + H^+ \rightarrow Fe^{3+} + \cdot OH + H_2O} \tag{12.8}$$

First of all, surface complex precursor was formed between $Fe^{3+}_{surf} - OH$ and H_2O_2 which may be considered as the initiation step (Eqs. 12.1–12.4). For the oxidation of organic pollutants, more number of hydroxyl radicals were needed which was produced by the dissociation of peroxide and reduction of Fe by interface electron transfer (Eqs. 12.5–12.6). The amount of Fe^{2+} on the surface of catalyst was increased to 38.7% from 26.1%. At the same time, these cyclic reactions for Cu^{2+}/Cu^{+} and Fe^{3+}/Fe^{2+} were carried out under acidic circumstances (Eqs. 12.7–12.8). And it was observed that the combined effect of Cu and Fe in the above reaction became very helpful in enhancing the hydroxyl radical production for the degradation of H_2O_2. It was also inferred from the above study that orange II was very well-attacked by Cu_2O (SO_4)-Fe_9 nanocomposite.

Another researcher Mai et al. reported the AOP reaction of Fenton system modified with Fe_2O_3 and $NaHSO_3$. This novel nanocomposite showed a very well-organized synergistic effect for the removal of Orange II and azo dye. In this study, the radical species produced were %OH and $\%SO_4^-$ showing very high competence to oxidize and degrade organic contaminants. In this concern, hydroxyl radical was formed by activating $NaHSO_3$ with Fe^{3+} reduced to Fe^{2+}. The removal efficiency was found to be 90% in 20 min when the pH was adjusted between 8 and 10. The experimental result and the pathways of the experiment are shown by the following equations.

$$\mathrm{\equiv Fe^{3+} + HSO_3^- + OH^- \rightarrow \equiv Fe^{2+} + \cdot SO_3^- + H_2O} \tag{12.9}$$

$$\cdot SO_3^- + \cdot O_2 \rightarrow SO_5^- \tag{12.10}$$

$$\cdot SO_5^- + 2 \equiv Fe^{2+} + H_2O \rightarrow 2 \equiv Fe^{3+} + \cdot SO_4^- + OH^- \tag{12.11}$$

$$\cdot SO_5^- + HSO_3^- \rightarrow \cdot SO_4^- + \cdot SO_4^{2-} + H_2O \tag{12.12}$$

$$\cdot SO_3^- + Fe^{2+} + H^+ \rightarrow Fe^{3+} + HSO_3^- (pH < 6) \tag{12.13}$$

$$\cdot SO_4^- + Fe^{2+} \rightarrow Fe^{3+} + SO_4^{2-} \tag{12.14}$$

$$\cdot OH^- + Fe^{2+} \rightarrow Fe^{3+} + OH^- \tag{12.15}$$

$$\cdot SO_4^- + HSO_3^- \rightarrow \cdot SO_3^- + SO_4^- + H_2O \tag{12.16}$$

$$\cdot SO_4^- + \cdot SO_4^- \rightarrow S_2O_8^{2-} \rightarrow 2SO_4^{2-} \tag{12.17}$$

$$\cdot SO_3^- + \cdot SO_3^- \rightarrow S_2O_6^{2-} \rightarrow 2SO_3^{2-} \rightarrow 2SO_4^{2-} \tag{12.18}$$

First of all, HSO_3^- was accumulated on Fe_2O_3 catalyst surface and it was studied under both acidic and alkaline conditions (Eq. 12.9). The $\cdot SO_3^-$ which was supported by dissolved oxygen generated the powerful oxidizing peroxy-sulfate ion $\cdot SO_5$ (Eq. 12.10) which was further reacted to Fe^{2+} along with HSO_3 (Eqs. 12.11–12.12) generating the stability and catalytic activity. This overall mechanism of degradation by $\cdot SO_4$ and $\cdot OH$ was found to be more consistent for Orange II with the formation of organic intermediates along with CO_2 and H_2O.

The core–shell nanocomposites of $Fe@Fe_2O_3$ were synthesized by Yang et al. for the degradation of Orange II dye. This heterogeneous catalyst was found to be very effective in the reaction of Fenton to degrade organic pollutants as well as dyes [44]. The efficiency of this nanocomposite was increased when this $Fe@Fe_2O_3$ was assisted by $NaHSO_3$. This combined form of the experimental nanocomposite was inferred for the removal of Orange II dye in both acidic as well as in alkaline medium. The mechanism of degradation process is shown below.

$$\equiv Fe^{3+} + 2HSO_3^- + 2OH^- \rightarrow \equiv Fe^{2+} + 2SO_3^{-\cdot} + H_2O \tag{12.19}$$

$$SO_3^{-\cdot} + O_2 \rightarrow \cdot SO_5^{-\cdot} \tag{12.20}$$

$$SO_5^{-\cdot} + HSO_3^- \rightarrow SO_4^{-\cdot} + SO_4^{2-} + H^+ \tag{12.21}$$

$$Fe^0 + 2Fe^{III} \rightarrow 3Fe^{II} \tag{12.22}$$

$$Fe^{II}OFe^{III} \rightarrow Fe^{III}OFe^{II} \tag{12.23}$$

$$Fe^{II}OFe^{III} + O_2 \rightarrow O_2^{-\cdot} \tag{12.24}$$

$$2O_2^{-\cdot} + 2H^+ \rightarrow H_2O_2 + O_2 \tag{12.25}$$

$$\equiv Fe^{2+} + H_2O_2 \rightarrow \equiv Fe^{3+} + OH^{\cdot} + OH^- \tag{12.26}$$

This process involves solid–liquid interface of $Fe@Fe_2O_3$ nanocomposites. First of all, the HSO_3^- radical species assembled on the surface of $Fe@Fe_2O_3$ catalyst. After that, SO_5^- was produced as a result of reaction of $\cdot SO_3^-$ and dissolved O_2^-. The $\cdot SO_5^-$ so obtained treated with HSO_3^- to obtain $\cdot SO_4$ (Eqs. 12.19–12.21). This Fenton catalyst could persuade electron transfer in between the Fe_2O_3 shell and Fe core which accelerated the generation of $\cdot O_2^-$ (Eqs. 12.22–12.24). The generation of radical resulted in the removal of Orange II. This mechanism was well-established for the removal of Orange II dye.

MgO/α-Fe_2O_3 nanocomposite was prepared by Allawi et al. with the help of hydrothermal process, and photo-oxidation operations were carried out for the degradation of MB dye. The study is mainly based on two assumptions i.e., (1) the decrease in recombination possibility of electron–hole pairs and (2) the increase in absorption of photon by MgO. So this study was made on combined photocatalytic outcome of MgO-Fe_2O_3 nanocomposite [45]. The mechanism of the reaction of as follows:

$$MgO/Fe_2O_3 + h\nu(\text{Vis Region}) \rightarrow MgO/Fe_2O_3\left(H^+ + e^-\right) \tag{12.27}$$

$$H^+ + H_2O(OH^{\cdot}) \rightarrow (OH^{\cdot}) + h^+ \tag{12.28}$$

$$h^+ + \text{Dye} \rightarrow \text{Dye}^{\cdot+}(\text{Oxidation of Dyes}) \tag{12.29}$$

$$e^- + O_2 \rightarrow O_2^{\cdot-} + \text{Semiconductor} \tag{12.30}$$

$$\text{Dye} + O_2^- \rightarrow \text{Degradation Products} \tag{12.31}$$

The result of degradation of MB dye was found to be 91.7% at pH 12 which was designated to be very cost-effective as well as efficient photocatalyst for mineralization of dye pollution.

Bouziani et al. synthesized the heterogeneous nanocomposite α-Fe_2O_3/TiO_2 by sol–gel method to integrate the photocatalytic activity of titanium oxide. The α-Fe_2O_3/TiO_2 nanocomposite showed great photocatalytic efficiency for the degradation of methylene blue i.e., 90% in 180 min of photo-illumination [46]. The process involved the generation of active species like ·OH, $\cdot O_2^-$, holes. The mechanism of the process is:

$$\mathrm{TF6} + h\nu \rightarrow \mathrm{TF6}\left(h^+ + e^-\right) \tag{12.32}$$

$$\mathrm{O_2} + e^- \rightarrow \mathrm{O_2^{-\cdot}} \tag{12.33}$$

$$\mathrm{O_2^{-\cdot}} + \mathrm{H^+} \rightarrow \mathrm{HO_2^{\cdot}} \tag{12.34}$$

$$2\mathrm{HO_2^{\cdot}} \rightarrow \mathrm{O_2} + \mathrm{H_2O_2} \tag{12.35}$$

$$\mathrm{H_2O_2} + \mathrm{O_2^{-\cdot}} \rightarrow \mathrm{OH^{\cdot}} + \mathrm{OH^-} + \mathrm{O_2} \tag{12.36}$$

$$\mathrm{H_2O_2} + h\nu \rightarrow 2\mathrm{OH^-} \tag{12.37}$$

A well-organized photocatalyst for the decolorization of MB dye was studied by Hojamberdiev et al. The Porolas-Fe_2O_3 nanocomposite (1%) was prepared using the precursor iron nitrate which was more amorphous as compared to 7% of the same nanocomposite. The heterogeneous photodecomposition on the nanomaterial surface by UV photo-irradiation [47].

$$\mathrm{H_2O} \rightarrow \mathrm{H^+} + \mathrm{OH^-} \tag{12.38}$$

$$e^{\mathrm{CB}-} + \mathrm{O_2} \rightarrow \mathrm{O_2^{\cdot -}} \tag{12.39}$$

$$\mathrm{O_2^{\cdot -}} + \mathrm{H_{aq}^+} \rightarrow \mathrm{HO_2^{\cdot}} \tag{12.40}$$

$$\mathrm{HO_2^{\cdot}} + \mathrm{HO_2^{\cdot}} \leftrightarrow \mathrm{H_2O_2} + \mathrm{O_2} \tag{12.41}$$

$$h^{\mathrm{VB}+} + \mathrm{OH_{aq}^-} \rightarrow \mathrm{OH^{\cdot -}} \tag{12.42}$$

$$\mathrm{MB^{\cdot}} + \mathrm{MB^{\cdot +}} + \mathrm{O_2^{\cdot -}}, \mathrm{HO_2^{\cdot}}, \mathrm{H_2O_2}, \mathrm{OH^{\cdot -}} \rightarrow \text{Degradation Products} \tag{12.43}$$

Mohamed et al. studied a *Z*-scheme photocatalytic system which simulated the photosynthesis by recombination of charge carrier and having great redox capacities. They produced the Fe_2O_3/GO/WO_3 3*Z*-Scheme nanocomposite [48] which was seen

to be very effective for the decolorization of MB and CV dyes. The mechanism of the reaction in α-Fe_2O_3/WO_3 system includes the electron–hole generation under solar light. The photo-generated electrons and photo-generated holes lead to the increase in oxidizing and reducing abilities of Fe_2O_3 and WO_3. These radical species generated in this reaction were responsible for the degradation of organic pollutant like methylene blue. The result of this study revealed that the efficiency of this nanocomposite for the removal of MB was 95.4% in 120 min. This process was found to be a green synthesis of $Fe_2O_3/GO/WO_3$ nanocomposite with the utilization of solar light.

The nanocomposite Fe_2O_3/Graphene/CuO (FGC), which is known to be a visible photo-sensitive material was successfully synthesized by Nuengmatcha et al. using a very simple solvothermal method. In this context, the photocatalytic activity of FGC was evaluated for the removal of MB when the nanocomposite was subjected to act in presence of visible light. It was found that the nanocomposite showed very great efficiency as compared to other types of catalysts. Furthermore, the mechanism of photocatalytic property of this hybrid composite was also studied. The synthesis of Fe_2O_3/graphene/CuO (FGC) [49] photocatalyst in a visible light system showed very good photocatalytic activity and brilliant magnetic separation capability. This method was very well-established for the removal of MB dye with an efficiency of more than 90% in 5 cycles. When FGC nanocomposites were used as a catalyst the valence band (VB) electrons of CuO were shifted to its conduction band (CB). This excitation results in the generation of electron–hole pairs (e^-/h^+) that mainly cause the photocatalytic as well as a redox reaction. As grapheme showed brilliant electronic conductivity and possessed large surface area, it behaved as electron transporter and acceptor. These reacted with O_2 which was dissolved in water and transformed to $O_2^{-\cdot}$ radical species. At the same time, the holes reacted to OH^-/H_2O absorbed on the surface of FGC to form ·OH. These radical species had a strong ability to oxidize and degrade MB to CO_2, H_2O with other byproducts. Following figure shows the mechanism of degradation of MB using this method.

Narendhran et al. [50] synthesized $Fe_2O_3/FeWO_4/WO_3$ nanostructures to examine the photocatalytic effect on methyl orange under UV–VIS irradiation method. When the nanoparticles were exposed to visible light, the band intensity of absorbed dye decreased. The hetero compound showed an efficiency of 98% within 160 min which was very high as compared to the individual reagents. These nanoparticles were synthesized by hydrothermal and precipitation method and no surfactant was added in the synthesis process. Santana et al. [51] synthesized a Fenton-like nanocomposite i.e., Fe_2O_3/MCM-41 for the photocatalytic degradation of methyl orange it showed a degradation efficiency of 70% in 120 min. The reaction mechanism of this reaction was as that of Fenton-like process which involves the production of hydroxyl radicals from hydrogen peroxide (H_2O_2) along with non-selective and highly oxidative OH radicals. These OH radical species showed brilliant efficiency toward degradation of organic pollutant like methyl orange. This study shows that Fe_2O_3/MCM-41 catalyst showed promising approach for the removal of MB dye.

Friendy and Sillanpaa synthesized a novel α-Fe_2O_3/Graphene nanomaterial for the removal of Rhodamine B (RhB) by visible light. α-Fe_2O_3/Gr nanocomposite [30] showed a brilliant catalytic activity with 98% toward the degradation of RhB under visible light. The series of disintegration process was performed to evaluate the reusability of the photocatalyst. This overall study showed that the nanocomposite was very effective, efficient, reusable, and eco-friendly. A novel nanocomposite was reported by Ouachtak et al. [12] for the adsorption of Rhodamine B by co-precipitation method and the nanocomposite was named as ν-Fe_2O_3@Mt or magnetic montmorillonite nanostructure. The adsorption property of RhB on ν-Fe_2O_3@Mt surface was measured. It was well-fitted with a great efficiency for the removal of RhB.

Jasmindar et al. [52] prepared a mesoporous Fe_2O_3/g-C_3N_4 nanomaterial for the removal of RhB. This novel nanocomposite showed an efficiency of 94.7% catalytic activity in 140 min. Due to the porous nature of Fe_2O_3/g-C_3N_4 monoliths, with higher charge separation ability, this leads to increase the catalytic property. This nanocomposite was found to be very effective and reusable. However, the nanocomposite was found to be very difficult to synthesize. The mechanism of the reaction involved the formation of holes (h^+), superoxides ($O_2^{-\cdot}$), and hydroxide radical species. This radical was used to decolorize the harmful RhB dye. Following figure shows the mechanism of the proposed reaction.

Another researcher Yang and Li studied the ZnO/Fe_2O_3 nanomaterial for the degradation of RhB in presence of UV-Light. The nanocomposite was synthesized by co-precipitation method. It showed brilliant photocatalytic activity for the degradation of RhB [53] when applied to external magnetic field, the magnetic saturation was sufficiently high. And the nanocomposite was found to be very efficient, eco-friendly, and showed outstanding photocatalytic activity. The following figure shows the mechanism of the reaction. Hasan et al. prepared a Υ-Fe_2O_3 nanomaterial for the removal of malachite green. The process was carried out by polymerization of oxidative free radical with acrylamide monomer. The novel material PACT@Υ-Fe_2O_3 nanocomposite [54] was utilized on the removal of MG with an efficiency of 77% in 170.28 min. as the conventional methods for the removal of dyes were found to be due to excessive cost, a most favorable approach could be adopted for its moderate approach, easy-handling and low cost as well. The optimization of various kind of processes could be maintained by the association of central composite design with response to surface methodology. The experimental process concludes toward degradation of MG with an easy access.

Jiang et al. synthesized novel Fe_2O_3 hollow box with double shell structure for the adsorption of MG by template-engage process. This nanocomposite was formed from diatomite@FeOOH [55] using the diatomite@MnO_2 material by a very simple route. The mechanism involved the introduction of Fe_2O_3/H_2O_2 in the solution of MG under irradiation of visible light. The Fe_2O_3 nanostructures are uniformly spreaded on the framework which was found to be 100% efficient in 60 min for the removal of MG in presence of H_2O_2. It exhibited great catalytic efficiency even after 5 cycles. This implies the nanomaterial can be taken as one of the promising catalysts used for the degradation of MG. Dehbi et al. used iron oxide nanoparticle from Fe $(NO_3)_3 \cdot 9H_2O$

and NH_4OH for the removal of malachite green (MG). The elimination efficiency was found to be 86.13% in 45 min using iron oxide. The nanocomposite was seen to be very recognized by thermodynamics stability. This α-Fe_2O_3 nanocomposite [56] was used as an efficient photocatalyst for the removal of MG.

Again another researcher introduced the application of Υ-Fe_2O_3 nanocomposite [57] for the removal of BTEX. The process was followed by photocatalytic degradation of semiconductors by gaining energy of the electrons present in the valence band (VB) and excited to CB. These electron–hole pairs (e^- and h^+) and hydroxyl radical were used for the degradation of BTEX in simpler compounds. The Υ–C nanomaterial was found to be very useful, cost-effective, and eco-friendly for the removal of BTEX. Ismail et al. [58] reported a very simple process to synthesize very efficient photocatalyst i.e., CNT-α-Fe_2O_3 nanocomposite for the removal of Bismarck Brown R dye (BBR). This nanomaterial showed an effectiveness of 98% for dye degradation when there was a synergistic effect of CNT and Fe_2O_3 interface. The main purpose of this study was to prepare an efficient photo-active mesoporous nano hybrid such as CNT-α-Fe_2O_3 with high sensitivity toward UV–VIS light. This nanomaterial can also be used as electrochemical sensor electrode. The photocatalyst showed remarkable efficiency for the removal of BBR dye.

Ghaffari et al. studied the AOPs for degrading organic dyes from wastewater. The process was followed by photocatalysis of fenton reactions with a very high efficiency. This involved a combined nanocomposite of Fe_2O_3/Mn_2O_3 [59] fabrication using the method of surfactant mediated co-precipitation. The recyclability was seen for seven cycles of catalytic reaction. The organic dye removal onto FMNC was found to be very efficient and sensitive for UV–VIS light.

Chen et al. [60] proposed a novel nanostructure for the degradation of organic contaminants which was a functionalized biochar of Fe_2O_3/TiO_2 (Fe_2O_3/TiO_2-BC). The preparation of the composite involves pyrolysis process, and the removal process involves oxidation and fenton-like reaction. In this context the MB (75%), RhB (60%) and MO (40%) were removed. Overall this system possesses brilliant potential for the degradation of organic pollutants. Liu et al. [61] reported a novel nanocomposite such as α-Fe_2O_3 having a silkworm–cocoon structure with brilliant adsorption capacity of 99.2–100% efficiency in the removal of several heavy metals along with various organic dyes such as CR, MO, etc. In this study, simple hydrothermal process to synthesize the nanocomposite and fenton-like photo-catalysis for the degradation of organic pollutants. This catalyst was well organized and possess high efficiency in the removal process even if at very low temperature and concentration. The overall study became very promising, cost-effective adsorbent for wastewater treatment. A hierarchically structured nanocomposite of Υ-Fe_2O_3-PPy [62] was prepared by Gopal et al. for the decolorization of cationic and anionic dyes. It was known to be an eco-friendly, low cost, and earth abundant composite for removing MB. These Υ-Fe_2O_3 nanocomposites possess very strong magnetic properties, high adsorption ability, and high surface area. This eco-friendly Fe_2O_3-PPy nanostructure was applied successfully in the removal of organic dyes.

12.3 Removal of Pesticides and Other Organic Pollutants

Along with the rapid progress of urbanization and industrialization, environmental pollution also increases rapidly. The wastewater from the developing industries is discharged into the water bodies, which contain different organic pollutants. Among them, different kinds of organic pollutants, such as pharmaceutical products, phenols, benzene compounds, antibiotics, and halogenated hydrocarbons, are toxic and harmful. Thus, it is necessary to discover an eco-friendly and high-productivity method to change organic pollutants into non-toxic and harmless products.

Singh et al. investigated the monolithic catalyst for the removal of industrial pesticides and dyes through a photo-Fenton-like system. This process involved the advanced oxidation process with the generation of hydroxyl radical (·OH) radical resulted in the degradation of pesticides as well as dyes. The novel nanocomposites formed in this process were Fe_2O_3/TiO_2 [63]. The mechanism of the system was found to be as like fenton system with the wide generation of various radical species. The nanocomposite obtained in this process was very cost-effective, non-toxic, and chemically stable in nature. It showed 95.7% efficiency in 150 min for reactive brilliant red X-33 dye and the herbicide 2,4-dichlorophynoxyacetic acid was removed with an efficiency of 18% in 1 h. Sun et al. [11] investigated the degradation of organic pollutant using a magnesium Mg-dopped $CuO–Fe_2O_3$ nanomaterials. Mg doping increased the catalytic activity of novel nanocomposite and the efficiency for degradation of phenol was found to be 84.36% in 45 min using 3.2% Mg doped $CuO-Fe_2O_3$ nano sheet modified with persulfate system (PS). This novel nanocomposite was prepared by hydrothermal method and inferred to be a cost-effective and eco-friendly photocatalyst.

Salari et al. reported the photocatalytic degradation of organic pollutant in aqueous solution under UV–VIS light. In this contest, the $Fe_2O_3/MoO_3/AgBr$ nanocomposite [64] was prepared by facile method. Various parameters such as amount of photo-catalyst calcinations temperature, dye concentration pH of the solution, and contact time were observed. It was inferred that the photocatalytic activity was increased with maximum peak at pH = 6.5. The experiment followed Langmuir Hinshelwood isotherm and Pseudo-first-order kinetics. Guo et al. [65] synthesized Ca-doped-Fe_2O_3 nanocomposites and used for the degradation of organic pollutants. They prepared low cost and environment-friendly calcium-doped α-Fe_2O_3 (Ca-Fe_2O_3) with abundant oxygen vacancies by precipitation method and used for the degradation of Rhodamine B (RhB). RhB was efficiently degraded by the 5% Ca-Fe_2O_3/PMS system over a pH values of (3.0–10.0), and the catalyst shows good constancy, flexibility, and less iron leaching. They reported that the process fitted well with the pseudo-first-order kinetics model.

Huang et al. synthesized magnetic $CuS/Fe_2O_3/Mn_2O_3$ nanocomposite via a facile Strategy and investigated the degradation of peroxymonosulfate (PMS) for ciprofloxacin (CIP) from aqueous solution. They reported that the magnetic CuS/Fe_2O_3/Mn_2O_3 nanocomposite [66] possessed higher catalytic activity for degradation of ciprofloxacin than bare CuS and Fe_2O_3/Mn_2O_3 composite. The degradation

process of ciprofloxacin was best fitted with the pseudo-first-order kinetic model and the highest rate was reached 0.10083 min^{-1} at the optimized conditions i.e., catalyst doses 0.6 $g{\cdot}L^{-1}$, PMS of 0.6 $g{\cdot}L^{-1}$, pH of the solution 5.84, initial concentration of 0.2 $g{\cdot}L^{-1}$ and time 120 min, the degradation efficiency was reported to be 88 and 48.6% corresponding to degradation and mineralization of ciprofloxacin, respectively. Ahmed et al. [67] studied the removal of Ciprofloxacin from wastewater via Pickering Emulsion Liquid Membrane Stabilized by Magnetic Nano-Fe_2O_3. They prepared the nanocomposite by ultrasonication for adsorption of Ciprofloxacin. They investigated the high rate of adsorption reached to 98.85% and minimum emulsion crack of 0.06% within 10 min addition time taken at the optimal operating conditions: 12,700 rpm homogenizer speed, 0.7 (%w/v) nano-Fe_2O_3 particles concentration, 6% (v/v) TBP concentration at emulsification time of 7 min and 0.1 M HCl in the internal phase.

Anfar et al. [68] prepared the Fe_2O_3/biochar by the process of green synthesis in microwave. They investigated the adsorption under different experimental parameters time (0–120 min), initial concentration (10–500 mg/L), pH (2–12). They reported the ultrasound-assisted adsorption capacity of salicylic acid, naproxen, and ketoprofen (SA, Nap, and Keto) from wastewater. For the removal (adsorption) of SA, Nap, and Keto the fitted kinetics and isotherm are pseudo-second-order model and Langmuir isotherm and maximum adsorption rate of SA, Nap, and Keto reaches to 683, 533, and 444 mg g^{-1}, respectively. Ding et al. [69] studied the degradation of salicylic acid from wastewater by using the α-Fe_2O_3/MXene. They prepared α-Fe_2O_3/MXene by facile hydrothermal method which is good degradation of salicylic acid from wastewater. The degradation rate of salicylic acid was reported 97% at 0.2 g/L FM-2 catalyst (17.1 wt.% of α-Fe_2O_3 loading) and 0.2 g/L PMS under neutral conditions.

Niu et al. [70] synthesized persulfate activated with magnetic γ-Fe_2O_3/CeO_2 by oxidation-precipitation method. They reported effective removal of tetracycline from wastewater by degradation process. They investigated γ-Fe_2O_3–CeO_2 had high crystallinity and good magnetism which leads good removal efficiency of tetracycline. The percentage of removal of tetracycline was reached to 84% under condition of a wide pH application range (pH 3–pH 9). Shan et al. synthesized magnetically recyclable $La_2O_2CO_3$/γ-Fe_2O_3 by using calcinating La-Fe binary MOF precursors as an adsorbent. They examined the adsorption of phosphate from wastewater by $La_2O_2CO_3$/γ-Fe_2O_3 [71]. Batch adsorption experiments showed that $La_2O_2CO_3$/γ-Fe_2O_3 (2:1) adsorbent exhibited a remarkable phosphate sorption capacity of 134.82 mg P/g, a fast sorption kinetic, strong selectivity for phosphate in the presence of co-existing anions, and a wide applicable pH range of 3–9. They reported the adsorption rate reached to 83.1%. Experimental data showed that the adsorption process followed Langmuir model and kinetics followed pseudo-second-order.

Wang et al. [10] prepared γ-Fe_2O_3@BC by pyrolysis of the pomelo peel-based biochar at a temperature of 400 °C and loaded with γ-Fe_2O. They studied the adsorption of norfloxacin from wastewater by using γ-Fe_2O_3@BC. The experimental study revealed that adsorption of norfloxacin followed the pseudo-second-order kinetic model. Again the experimental study confirmed the adsorption isotherm followed the Sips mode. García-Muñoz et al. investigated the wastewater treatment

by removing norfloxacin via degradation. They used mesoporous Fe_2O_3–TiO_2 [72] for the wastewater treatment which was prepared via structure-directing-surfactant method. They reported the best results were obtained with catalysts that had a surface Fe_2O_3 content of 3% (w/w), where the breakdown of H_2O_2 led to the maximum norfloxacin running down rate. They examined using 405 nm LED light, Fe_2O_3–TiO_2 improved the process efficiency and under UV illumination at 405 nm and with a stoichiometric amount of H_2O_2, almost complete norfloxacin removal and almost total mineralization were achieved in 120 min at 298 K and pH = 7.

Abdel-Wahab et al. [73] studied the treatment of pharmaceutical wastewater containing paracetamol by the help of magnetic flower-like TiO_2/Fe_2O_3 core–shell. They synthesized the magnetic flower-like TiO_2/Fe_2O_3 core–shell nanocomposite which was ultrasonically assisted by sol–gel method with some alterations. They mentioned that paracetamol was completely degraded after 90 min with 50% TiO_2/Fe_2O_3 under light irradiation and 66% paracetamol mineralization had occurred. They investigated the attack of the –OH radical on the aromatic ring which was supposed to be the initial point for photo-degradation of paracetamol. By experimental data, the kinetics study indicated that degradation fitted with pseudo-first-order reaction. Chahm et al. [74] reported the adsorption of ibuprofen from wastewater with the help of O-carboxymethyl-N-laurylchitosan/γ-Fe_2O_3. For the adsorption mechanism, they studied Langmuir, Freundlich, and Sips isotherms and kinetics of pseudo-first-order, pseudo-second-order, and intra-particle diffusion model. They reported the maximum adsorption of ibuprofen was found to be 395 mg/g at 25 °C and pH 7.0 which was well-fit for Sips isotherms and pseudo-second-order kinetics.

Lin et al. investigated the treatment of wastewater by using $Ag/TiO_2/Fe_2O_3$. They reported the removal of deleterious and recalcitrant compounds by using this novel nanoparticle [75]. The maximum TOC removal at optimum conditions of light wavelength (254 nm), pH (4.68), photocatalyst dosage (480 mg/L), and initial TOC concentration (11,126.5 mg/L) was calculated using a numerical optimization approach of 9.78% and validated with experimental results of 9.42%. Ding et al. [76] studied the anode and cathode of an electrochemical/electro-Fenton oxidation (EC/EF) device to degrade atrazine were boron-doped diamond (BDD) and Fe@Fe_2O_3 core–shell nanowires loaded active carbon fiber (Fe@Fe_2O_3/ACF), respectively. Fe@Fe_2O_3 could activate molecular oxygen 31 to produce more ·OH via Fenton reaction, preferring atrazine degradation, according to an active 30 species trapping experiment.

He et al. [77] were studied the treatment of municipal wastewater. They prepared Fe@Fe_2O_3 nanomaterial combined with polydiallyldimethylammonium chloride (PDMDAAC) and H_2SO_4 for sludge dewatering and found that the nanocomposite was very effective. Cao et al. studied the wastewater treatment which contains refractory pollutants via adsorption and catalytic oxidation. They performed the adsorption experiment by use of γ-Fe_2O_3/Bentonite [78] Modified which was prepared via a facile and eco-friendly reaction. They investigated the removal of BPA (bisphenol A). The experimental data showed that Langmuir isotherm well-fitted with adsorption with adsorption capacity of 77.36 mg/g. BPA photocatalytic degradation by product had a reaction rate constant of 0.00104 min^{-1}. They reported the catalytic activity

of the material still reached 91% after 5 experiment repeatedly. Pan et al. examined the degradation of bisphenol A (BPA) from wastewater. They used Aldehyde-modified *a*-Fe_2O_3/graphitic carbon nitride (α-Fe_2O_3-DBD/g-C_3N_4) [79] prepared by complexation reaction for the degradation of bisphenol A. They reported under 180 min of photocatalytic irradiation, the mineralization rate of BPA over 1.6% and α-Fe_2O_3-DBD/g-C_3N_4 was 52.2%, which is 6.14 times higher than that over g-C_3N_4.

Gao et al. synthesized heterogeneous Fenton-like catalyst which was used to treat the wastewater. By the use of sol–gel technique and sufficient oxygen vacancies (OVs) promoted the synthesis of Fe_2O_3–CeO_2 photocatalyst. They degraded sulfamerazine from wastewater with an efficient manner. They reported that the Fe_2O_3–CeO_2 catalyst [80] was confirmed to have very good activity and stability after 75 min at pH 3.0 and temperature 45 °C in an Oxygen atmosphere and in these conditions, the Fenton-like reaction achieved complete SMR conversion. The main active species of the reaction were surface-bound OH radicals. In the Fenton-like method, OVs on the surface of the Fe_2O_3–CeO_2 catalyst highly improved the formation of OH under the atmosphere of O_2. Huo et al. [81] developed *Z*-scheme α-Fe_2O_3/MIL-101(Cr) hybrid materials for the treatment of wastewater under the irradiation of UV–VIS light. They reported the degradation of carbamazepine from contaminated water. They prepared the *Z*-scheme α-Fe_2O_3/MIL-101(Cr) structure via hydrothermal method. The experimental data indicated that the carbamazepine was completely adsorbed from contaminated water after 180 min irradiation over the optimum α-Fe_2O_3 (0.3)/MIL-101(Cr) hybrid.

Yan et al. studied the treatment of wastewater by removing nitrobenzene from aqueous solution. The degradation of nitrobenzene was done by preparing Si-doped α-Fe_2O_3 nanocomposites [82]. The adsorption experiment suggested that pH of the solution is 6.5. They reported best Si/Fe ratio of Si-doped α-Fe_2O_3 catalyst was 0.5 in present and suggested that a heavy dose of Si-doped α-Fe_2O_3 makes high removal of nitrobenzene. Gao et al. [83] studied degradation of phenol from wastewater by using magnetic Fe_2O_3–ZrO_2. They synthesized the nanocomposite by sol–gel method. Hydroxyl and superoxide radicals were generated by the Fe_2O_3–ZrO_2 photocatalyst they reported. In the heterogeneous system, complete phenol conversion and 56% TOC removal were attained after 210 min at 60 °C at neutral pH. Wang et al. investigated the degradation of 4-chlorophenol and 4-nitrophenol for the treatment of wastewater. They prepared the nanocomposite oleophilic Fe_2O_3/polystyrene fibers [84] via electrospinning and γ-Ray irradiation methods. The photocatalytic degradation of 4-CP and 4-NP were stated to be 80 and 75% in the 6th cycling and the composite fiber showed the batter recyclability of about 90%. Salih et al. [85] prepared the hematite (α-Fe_2O_3) nanocomposite by a modified method i.e., solution combustion and applied for the degradation of pollutants present in petroleum refinery wastewater using hematite (α-Fe_2O_3) and reported the biodegradability rate of BOD/COD was increased from 0.074 to 0.604. The removal rate was observed to be 90.85% for 90 min at a catalyst concentration of 5 gL^{-1}, pH of 7.5, and H_2O_2/COD ratio of 1 mg g^{-1} (Table 12.1).

Table 12.1 Removal capacity of different materials

Materials	Organic contaminant	Process of removal	pH	Maximum removal capacity	Author
Peroxymonosulfate activated CuS/Fe_2O_3/Mn_2O_3 Magnetic nanocomposite	Ciprofloxacin	Degradation	5.8	88%	[66]
α-Fe_2O_3/$Cu_2O(SO_4)$ composite	Orange II	Degradation	3.5	98.9%	[43]
Maghemite nanoparticles (γ-Fe_2O_3-NPs)	Textile and tanning wastewater effluents	Degradation	–	89.4%	[86]
Polyethersulfone-maghemite (PES/γ-Fe_2O_3) composite membranes	Oil–water mixtures	Self-cleaning and anti-fouling	–	81.7%	[13]
Fe_2O_3/Mn_2O_3	Organic dyes	Photodegradation	–	80–97%	[59]
A three-dimensional electrochemical oxidation system with a—Fe_2O_3/PAC	Ammonium nitrogen	Degradation	–	95.30%	[87]
Fe_2O_3/biochar	Nonsteroidal Anti-inflammatory Drugs (NSAIDs) (salicylic acid, naproxen, and ketoprofen)	Adsorption	3.2	Salicylic acid (99.52%), Naproxen (95.86%), and Ketoprofen (93.45%)	[68]
Haematite α-Fe_2O_3	Pollutants present in Petroleum refinery	Photocatalytic degradation	–	90.85%	[85]
MgO/α-Fe_2O_3 Nanocomposite	Methylene Blue	Degradation	12	91.7%	[45]
Fe_2O_3/TiO_2 functionalized biochar	Dye	Degradation	6	65%	[60]
Novel α-Fe_2O_3/MXene nanocomposite	Salicylic acid	Degradation	7.4	97%	[69]
α-Fe_2O_3/graphene	RhB	Degradation	–	~ 98%	[30]
Hierarchically structured γ-Fe_2O_3-PPy	Cationic dye	Adsorption	11	98%	[62]
Polyacrylamide-g-chitosan γ-Fe_2O_3 nanocomposite	Malachite green	Filtration	–	73%	[54]

(continued)

Table 12.1 (continued)

Materials	Organic contaminant	Process of removal	pH	Maximum removal capacity	Author
Fenton-like system of Fe_2O_3 and $NaHSO_3$	Orange II	Degradation	5	90%	[88]
$Fe_2O_3/WO_3/FeWO_4$	Methyl orange	Photocatalytic degradation	–	98%	[50]
Persulfate activated with magnetic γ-Fe_2O_3/CeO_2 catalyst	Tetracycline	Degradation	3–9	84%	[70]
Fe_2O_3	Anionic dye	Adsorption	3		[89]
Magnetic montmorillonite composite γ-Fe_2O_3@Mt	Rhodamine B dye	Adsorption	5.5		[12]
Fe_2O_3/MCM-41	Methyl orange	Degradation			[51]
Mesoporous magnetic Fe_2O_3/g-C3N4 monoliths	Rhodamine B	Degradation	7	94.7%	[52]
Mg doped CuO-Fe_2O_3 composites	Organic pollutants	Degradation	3–11	84.36%	[11]
γ-Fe_2O_3@BC	Norfloxacin	Adsorption	3–5	61.43%	[10]
Mn_3O_4–FeS_2/Fe_2O_3	Orange II	Degradation	2.8	99.0%	[90]
Magnetic flower-like TiO_2/Fe_2O_3 core–shell	Paracetamol	Photocatalytic degradation		100%	[73]
O-carboxymethyl-Nlaurylchitosan/ γ-Fe_2O_3	Ibuprofen	Adsorption	7	99%	[74]
Magnetic Fe_2O_3–ZrO_2	Phenol	Degradation	7	56%	[83]
Fe_2O_3 nano sheet	Malachite green	Degradation		99.9%	[55]
$Ag/TiO_2/Fe_2O_3$	Confectionery wastewater	Degradation	4.68	9.24%	[75]

(continued)

Table 12.1 (continued)

Materials	Organic contaminant	Process of removal	pH	Maximum removal capacity	Author
α-Fe_2O_3	Congo red (CR), methyl orange (MO)	Adsorption	–	99.2 and 83.9%	[61]
ZnO/Fe_2O_3	Rhodamine B	Degradation	–	97.6	[53]
Magnetic γ-Fe_2O_3/CeO_2	Tetracycline	Degradation	3–9	84%	[70]
Fe_2O_3	COD	Electro-Fenton process	2.84	67.65	[91]
Fe@Fe_2O_3/ACF	Atrazine	Degradation	3	100	[76]
Fe@Fe_2O_3/H_2SO_4/PDMDAAC	Sludge dewatering	Degradation	2.9	78.1	[77]
Fe_2O_3/MoO_3/AgBr	Organic pollutant	Degradation	6.5	60%	[64]
Fe@Fe_2O_3	Orange II	Degradation	3	90%	[44]
Mesoporous Fe_2O_3–TiO_2	Norfloxacin	Degradation	7	60%	[72]
α-Fe_2O_3/TiO_2	Methylene Blue (MB) and Phenol (Ph)	Degradation		90% of MB and 50% of Ph	[46]
γ-Fe_2O_3/Bentonite Modified	Bisphenol A (BPA)	Adsorption	2–6	91%	[78]
α-Fe_2O_3/Carbon Nanotubes	Bismarck Brown R (BBR) Dye	Adsorption		98%	[58]
α-Fe_2O_3	Malachite green	Adsorption		86.13%	[56]
Fe_2O_3–CeO_2	Sulfamerazine	Degradation	3	100%	[80]
Ca-doped—Fe_2O_3	Organic pollutants	Degradation	3.0–10.0	91, 99 and 99%	[65]
Amorphous Fe_2O_3	Methylene blue (MB)	Adsorption		96–98%	[47]
Z-scheme α-Fe_2O_3/MIL-101(Cr) hybrid	Carbamazepine	Degradation		100%	[81]
γ-Fe_2O_3/α-MnO_2	Organic contaminant (Rhodamine B)	Adsorption	5.27	92.79%	[92]
Cu-doped Fe@Fe_2O_3	Tetracycline	Degradation	3.0–4.0	98.1%	[93]

(continued)

Table 12.1 (continued)

Materials	Organic contaminant	Process of removal	pH	Maximum removal capacity	Author
Fe_2O_3/GO/WO_3	MB and CV and phenol	Degradation		95.4% of phenol	[48]
Magnetic Nano-Fe_2O_3	Ciprofloxacin	Adsorption	8	98.85%	[67]
Fe_2O_3/graphene/CuO	Methylene blue	Degradation	1–11	78.80%	[49]
α-Fe_2O_3-DBD/g-C_3N_4	Bisphenol A	Degradation			[79]
magnetic Fe_2O_3	Lead ions	Adsorption	3	97.2%	[94]
γ-Fe_2O_3	COD	Degradation	2–8	90.94%	[57]
Fe_2O_3/TiO_2	Industrial dye and pesticide (RbX)	Degradation	3	88.71%	[63]
Oleophilic Fe_2O_3/polystyrene fibers	4-chlorophenol and 4-nitrophenol	Degradation	4.3	80 and 75%	[84]
Si-doped α-Fe_2O_3	Nitrobenzene	Degradation	6.5		[82]

12.4 Conclusion

This chapter explains the recent investigations on photocatalytic degradation of various organic as well as azo dyes. The decoration of these dye particles has been found to be very well-established due to the large surface area of iron oxide nanocomposite and its magnetic properties. To give a superior comprehension of the impact of various photocatalytic frameworks and the impact of planning methods on morphological properties for improved iron oxide execution, general data on photocatalytic corruption, a few instances of the Fenton oxidation process, and different amalgamation courses of various morphologies of iron oxide have been incorporated. To sum up, utilizing appropriate help materials, a very scattered photocatalyst with a high surface region, abundant dynamic destinations, and better contamination particle adsorption could be understood. Moreover, acquiring a useful old-style heterojunction or *Z*-plot heterojunction requires a cautious choice of a semiconductor photocatalyst with a sufficient band hole to be combined with iron oxide. The expanded reaping of noticeable light because of diminished band holes decreased charge recombination, and more successful charge transporter partitions show that both heterojunctions were well planned. However, it's actually quite important that there are still a large number of associated concerns and examination chances to be investigated in the future. To the best of our knowledge, there hasn't been any exploration of surface imperfections like oxygen opportunities and metal blemishes for further developing Fe_2O_3 performance. Several studies have been distributed to date on the examination of deformity areas for adjusting the band hole while supporting charge division and, in this manner, helping photocatalytic performance. Both metal deformities and oxygen opening can change the electronic band structure by shaping mid-hole states beneath the CB, modifying the band hole energy for apparent light gathering and charge transporter detachment at the same time. Several methods have been accounted for producing imperfection locales, including warming under vacuum or at high temperatures, illuminating with UV, lessening treatment, plasma-treating, and so on. Furthermore, the expansion of an alternate valence-state metal dopant would bring about the development of surface defects. In different examinations, oxygen openings and metal imperfections were made on the outer layer of photocatalysts through a self-doping strategy without the utilization of any impurity materials, and disorganized layers were created.

References

1. Tornero V, Hanke G (2016) Chemical contaminants entering the marine environment from sea-based sources: a review with a focus on European seas. Mar Pollut Bull 112(1–2):17–38
2. León O, Muñoz-Bonilla A, Soto D, Pérez D, Rangel M, Colina M, Fernández-García M (2018) Removal of anionic and cationic dyes with bioadsorbent oxidized chitosans. Carbohydr Polym 194:375–383

3. Mohd Adnan MA, Muhd Julkapli N, Amir MNI, Maamor A (2019) Effect on different TiO_2 photocatalyst supports on photodecolorization of synthetic dyes: a review. Int J Environ Sci Technol 16(1):547–566
4. Pavithra KG, Jaikumar V (2019) Removal of colorants from wastewater: a review on sources and treatment strategies. J Ind Eng Chem 75:1–19
5. Cinperi NC, Ozturk E, Yigit NO, Kitis M (2019) Treatment of woolen textile wastewater using membrane bioreactor, nanofiltration and reverse osmosis for reuse in production processes. J Clean Product 223:837–848
6. Jusoh NWC, Jalil AA, Triwahyono S, Setiabudi HD, Sapawe N, Satar MAH, Karim AH, Kamarudin NHN, Jusoh R, Jaafar NF, Salamun N, Efendi J (2013) Sequential desilication-isomorphous substitution route to prepare mesostructured silica nanoparticles loaded with ZnO and their photocatalytic activity. Appl Catal A Gen 468:276–287
7. Brillas E, Martínez-Huitle CA (2015) Decontamination of wastewaters containing synthetic organic dyes by electrochemical methods: an updated review. Appl Catal B Environ 166:603–643
8. Bhattacharyya S, Das P, Datta S (2019) Removal of ranitidine from pharmaceutical waste water using activated carbon (AC) prepared from waste lemon peel. In: Ghosh SK (ed) Waste water recycling management. Springer, New York, pp 123–142
9. Wen B, Li J, Lin Y, Liu X, Fu J, Miao H, Zhang Q (2011) A novel preparation method for γ-Fe_2O_3 nanoparticles and their characterization. Mater Chem Phys 128(1–2):35–38
10. Wang J, Zhang M, Zhou R, Li J, Zhao W, Zhou J (2020) Adsorption characteristics and mechanism of norfloxacin in water by γ-Fe_2O_3@BC. Water Sci Technol 82(2):242–254
11. Sun M, Lei Y, Cheng H, Ma J, Qin Y, Kong Y, Komarneni S (2020) Mg doped CuO–Fe_2O_3 composites activated by persulfate as highly active heterogeneous catalysts for the degradation of organic pollutants. J Alloys Comp 825:154036–154047
12. Ouachtak H, El Haouti R, El Guerdaoui A, Haounati R, Amaterz E, Addi AA, Akbal F, Taha ML (2020) Experimental and molecular dynamics simulation study on the adsorption of Rhodamine B dye on magnetic montmorillonite composite γ-Fe_2O_3@Mt. J Mol Liquids 309:113142–113160
13. Ouda M, Ibrahim Y, Banat F, Hasan SW (2020) Oily wastewater treatment via phase-inverted polyethersulfone-maghemite (PES/γ-Fe_2O_3) composite membranes. J Water Process Eng 37:101545–101555
14. Lai X, Guo R, Xiao H, Lan J, Jiang S, Cui C, Ren E (2019) Rapid microwave-assisted bio-synthesized silver/dandelion catalyst with superior catalytic performance for dyes degradation. J Hazard Mater 371:506–512
15. Jalil AA, Satar MAH, Triwahyono S, Setiabudi HD, Kamarudin NHN, Jaafar NF, Sapawe N, Ahamad R (2013) Tailoring the current density to enhance photocatalytic activity of CuO/HY for decolorization of malachite green. J Electroanal Chem 701:50–58
16. Chen X, Ji D, Wang X, Zang L (2017) Review on Nano zerovalent Iron (nZVI): from modification to environmental applications. In: IOP conference series on earth environment science, p 12004
17. Grégorio C, Eric L (2019) Advantages and disadvantages of techniques used for wastewater treatment. Environ Chem Lett 17:145–155
18. Lei C, Pi M, Jiang C, Cheng B, Yu J (2017) Synthesis of hierarchical porous zinc oxide (ZnO) microspheres with highly efficient adsorption of Congo red. J Colloid Interface Sci 490:242–251
19. Chen Y, Liu Y, Li Y, Wu Y, Chen Y, Liu Y, Zhang J, Xu F, Li M, Li L (2020) Synthesis, application and mechanisms of Ferro-Manganese binary oxide in water remediation: a review. Chem Eng J 388:124313–124327
20. Zhang F, Chen X, Wu F, Ji Y (2016) High adsorption capability and selectivity of ZnO nanoparticles for dye removal. Colloids Surf A Physicochem Eng Aspects 509:474–483
21. Zhang S, Li B, Wang X, Zhao G, Hu B, Lu Z, Wen T, Chen J, Wang X (2020) Recent developments of two-dimensional graphene-based composites in visible-light photocatalysis for eliminating persistent organic pollutants from wastewater. Chem Eng J 390:124642–124654

22. Bharathi D, Ranjithkumar R, Chandarshekar B, Bhuvaneshwari V (2019) Preparation of chitosan coated zinc oxide nanocomposite for enhanced antibacterial and photocatalytic activity: as a bionanocomposite. Int J Biol Macromol 129:989–996
23. Tao Q, Bi J, Huang X, Wei R, Wang T, Zhou Y, Hao H (2021) Fabrication, application, optimization and working mechanism of Fe_2O_3 and its composites for contaminants elimination from wastewater. Chemosphere 263:127889–127909
24. Kataria N, Garg VK (2018) Green synthesis of Fe_3O_4 nanoparticles loaded sawdust carbon for cadmium(II) removal from water: regeneration and mechanism. Chemosphere 208:818–828
25. Mosleh S, Rahimi MR, Ghaedi M, Dashtian K, Hajati S, Wang S (2017) Ag_3PO_4/AgBr/Ag-HKUST-1-MOF composites as novel blue LED light active photocatalyst for enhanced degradation of ternary mixture of dyes in a rotating packed bed reactor. Chem Eng Process Process Intens 114:24–38
26. Chauhan AK, Kataria N, Garg VK (2020) Green fabrication of ZnO nanoparticles using *Eucalyptus* spp. leaves extract and their application in wastewater remediation. Chemosphere 247:125803–125815
27. Yuan X, Zhou C, Jin Y, Jing Q, Yang Y, Shen X, Tang Q, Mu Y, Du AK (2016) Facile synthesis of 3D porous thermally exfoliated g-C_3N_4 nanosheet with enhanced photocatalytic degradation of organic dye. J Colloid Interface Sci 468:211–219
28. Li R, Jia Y, Bu N, Wu J, Zhen Q (2015) Photocatalytic degradation of methyl blue using Fe_2O_3/TiO_2 composite ceramics. J Alloys Comp 643:88–93
29. Pang Y, Li Z, Jiao X, Chen D, Li C (2020) Metal-organic framework derived porous α-Fe_2O_3/C nano-shuttles for enhanced visible-light photocatalysis. ChemistrySelect 5(3):1047–1053
30. Frindy S, Sillanpää M (2020) Synthesis and application of novel α-Fe_2O_3/graphene for visible-light enhanced photocatalytic degradation of RhB. Mater Des 188:108461–108473
31. Zhang H, Wei X, Liu L, Zhang Q, Jiang W (2019) The role of positively charged sites in the interaction between model cell membranes and γ-Fe_2O_3 NPs. Sci Total Environ 673:414–423
32. Sehlleier YH, Hardt S, Schulz C, Wiggers H (2016) A novel magnetically-separable porous iron-oxide nanocomposite as an adsorbent for methylene blue (MB) dye. J Environ Chem Eng 4(4):3779–3787
33. Othman NH, Alias NH, Shahruddin MZ, Abu Bakar NF, Nik Him NR, Lau WJ (2018) Adsorption kinetics of methylene blue dyes onto magnetic graphene oxide. J Environ Chem Eng 6(2):2803–2811
34. Amer R, Hadi H (2022) Application of CTAB-coated magnetic nanoparticles for solid-phase extraction of thiamine hydrochloride from pharmaceutical formulations and urine samples. Arab J Sci Eng 47:429–440
35. Kanwal A, Bhatti HN, Iqbal M, Noreen S (2017) Basic dye adsorption onto clay/$MnFe_2O_4$ composite: a mechanistic study. Water Environ Res 89(4):301–311
36. Ianoş R, Păcurariu C, Muntean SG, Muntean E, Nistor MA, Nižňanský D (2018) Combustion synthesis of iron oxide/carbon nanocomposites, efficient adsorbents for anionic and cationic dyes removal from wastewaters. J Alloys Compd 741:1235–1246
37. Lilhare S, Mathew SB, Singh AK, Carabineiro SAC (2021) Calcium alginate beads with entrapped iron oxide magnetic nanoparticles functionalized with methionine—a versatile adsorbent for arsenic removal. Nanomaterials 11(5):1345–1355
38. Ge YL, Zhang YF, Yang Y, Xie S, Liu Y, Maruyama T, Deng ZY, Zhao X (2019) Enhanced adsorption and catalytic degradation of organic dyes by nanometer iron oxide anchored to single-wall carbon nanotubes. Appl Surf Sci 488:813–826
39. Samrot AV, Ali HH, Selvarani J, Faradjeva E, Kumar S (2021) Adsorption efficiency of chemically synthesized superparamagnetic iron oxide nanoparticles (SPIONs) on crystal violet dye. Curr Res Green Sustain Chem 4:100066–100080
40. Rajabi M, Mahanpoor K, Moradi O (2019) Preparation of PMMA/GO and PMMA/GO-Fe_3O_4 nanocomposites for malachite green dye adsorption: kinetic and thermodynamic studies. Compos B Eng 167:544–555
41. Qiu Y, Xu X, Xu Z, Liang J, Yu Y, Cao X (2020) Contribution of different iron species in the iron-biochar composites to sorption and degradation of two dyes with varying properties. Chem Eng J 389:124471–124483

42. Kausar A, Bhatti HN, Iqbal M, Ashraf A (2017) Batch versus column modes for the adsorption of radioactive metal onto rice husk waste: conditions optimization through response surface methodology. Water Sci Technol 76(5):1035–1043
43. Guo X, Xu Y, Zha F, Tang X, Tian H (2020) α-Fe_2O_3/$Cu_2O(SO_4)$ composite as a novel and efficient heterogeneous catalyst for photo-Fenton removal of Orange II. Appl Surf Sci 530:1–11
44. Yang Y, Sun M, Zhou J, Ma J, Komarneni S (2020) Degradation of orange II by Fe@Fe_2O_3 core shell nanomaterials assisted by $NaHSO_3$. Chemosphere 244:125588–125600
45. Allawi F, Juda AM, Radhi SW (2020) Photocatalytic degradation of methylene blue over MgO/α-Fe_2O_3 nano composite prepared by a hydrothermal method. In: AIP conference on the proceedigns, pp 030020–030037
46. Bouziani A, Park J, Ozturk A (2020) Synthesis of α-Fe_2O_3/TiO_2 heterogeneous composites by the sol–gel process and their photocatalytic activity. J Photochem Photobiol A Chem 400:112718–112732
47. Hojamberdiev M, Kadirova ZC, Daminova SS, Yubuta K, Razavi-Khosroshahi H, Sharipov KT, Miyauchi M, Teshima K, Hasegawa M (2019) Amorphous Fe_2O_3 nanoparticles embedded into hypercrosslinked porous polymeric matrix for designing an easily separable and recyclable photocatalytic system. Appl Surf Sci 466:837–846
48. Mohamed HH (2019) Rationally designed Fe_2O_3/GO/WO3 Z-scheme photocatalyst for enhanced solar light photocatalytic water remediation. J Photochem Photobiol A Chem 378:74–84
49. Nuengmatcha P, Porrawatkul P, Chanthai S, Sricharoen P, Limchoowong N (2019) Enhanced photocatalytic degradation of methylene blue using Fe_2O_3/graphene/CuO nanocomposites under visible light. J Environ Chem Eng 7(6):103438–103458
50. Narendhran S, Shakila PB, Manikandan M, Vinoth V, Rajiv P (2020) Spectroscopic investigation on photocatalytic degradation of methyl orange using Fe_2O_3/WO_3/$FeWO_4$ nanomaterials. Spectrochim Acta A Molecul Biomolecul Spectrosc 232:118164–118171
51. Sidney Santana C, Freire Bonfim DP, da Cruz IH, da Silva Batista M, Fabiano DP (2021) Fe_2O_3/MCM-41 as catalysts for methyl orange degradation by Fenton-like reactions. Environ Prog Sustain Energy 40(2):1–9
52. Singh J, Basu S (2020) Synthesis of mesoporous magnetic Fe_2O_3/g-C_3N_4 monoliths for Rhodamine B removal. Microp Mesop Mater 303:110299–110307
53. Yang Y, Li X, Zhao R, Yang J, Sun Q, Chen X, Wu X (2018) The study on degradation and separation of RhB under UV light by magnetically ZnO/Fe_2O_3 nanoparticles. Phys Status Solidi A Appl Mater Sci 215(23):1–7
54. Hasan I, Bhatia D, Walia S, Singh P (2020) Removal of malachite green by polyacrylamide-g-chitosan γ-Fe_2O_3 nanocomposite-an application of central composite design. Groundwater Sustain Develop 11:100378–100390
55. Jiang D, Bin X, Liu X, Xu X, Zhang YX (2018) Double-shell Fe_2O_3 hollow box-like structure for enhanced photo-Fenton degradation of malachite green dye. J Phys Chem Solids 112:209–215
56. Dehbi A, Dehmani Y, Omari H, Lammini A, Elazhari K, Abdallaoui A (2020) Hematite iron oxide nanoparticles (α-Fe_2O_3): synthesis and modelling adsorption of malachite green. J Environ Chem Eng 8(1):103394–103410
57. Sheikholeslami Z, Kebria DY, Qaderi F (2020) Application of γ-Fe_2O_3 nanoparticles for pollution removal from water with visible light. J Molecul Liquids 299:1–10
58. Ismail AA, Ali AM, Harraz FA, Faisal M, Shoukry H, Al-Salami AE (2019) A facile synthesis of α-Fe_2O_3/carbon nanotubes and their photocatalytic and electrochemical sensing performances. Int J Electrochem Sci 14(1):15–32
59. Ghaffari Y, Gupta NK, Bae J, Kim KS (2020) One-step fabrication of Fe_2O_3/Mn_2O_3 nanocomposite for rapid photodegradation of organic dyes at neutral pH. J Molecul Liquids 315:113691–113707
60. Chen XL, Li F, Chen HY, Wang HJ, Li GG (2020) Fe_2O_3/TiO_2 functionalized biochar as a heterogeneous catalyst for dyes degradation in water under Fenton processes. J Environ Chem Eng 8(4):103905–103915

61. Liu H, Wang Z, Li H, Wang H, Yu R (2018) Controlled synthesis of silkworm cocoon-like α-Fe_2O_3 and its adsorptive properties for organic dyes and Cr(VI). Mater Res Bull 100:302–307
62. Gopal RA, Song M, Yang D, Lkhagvaa T, Chandrasekaran S, Choi D (2020) Synthesis of hierarchically structured ϒ-Fe_2O_3-PPy nanocomposite as effective adsorbent for cationic dye removal from wastewater. Environ Pollut 267:115498–115507
63. Singh J, Sharma S, Aanchal and S. Basu, (2019) Synthesis of Fe_2O_3/TiO_2 monoliths for the enhanced degradation of industrial dye and pesticide via photo-Fenton catalysis. J Photochem Photobiol A Chem 376:32–42
64. Salari H, Kohantorabi M (2020) Fabrication of novel $Fe_2O_3/MoO_3/AgBr$ nanocomposites with enhanced photocatalytic activity under visible light irradiation for organic pollutant degradation. Adv Powder Technol 31(1):493–503
65. Guo S, Wang H, Yang W, Fida H, You L, Zhou K (2020) Scalable synthesis of Ca-doped α-Fe_2O_3 with abundant oxygen vacancies for enhanced degradation of organic pollutants through peroxymonosulfate activation. Appl Catal B Environ 262:118250–118265
66. Huang Y, Chao Nengzi L, Zhang X, Gou J, Gao Y, Zhu G, Cheng Q, Cheng X (2020) Catalytic degradation of ciprofloxacin by magnetic $CuS/Fe_2O_3/Mn_2O_3$ nanocomposite activated peroxymonosulfate: Influence factors, degradation pathways and reaction mechanism. Chem Eng J 388:124274–124287
67. Mohammed AA, Atiya MA, Hussein MA (2020) Studies on membrane stability and extraction of ciprofloxacin from aqueous solution using pickering emulsion liquid membrane stabilized by magnetic nano-Fe_2O_3. Colloids Surf A Physicochem Eng Aspects 585:124044–124060
68. Anfar Z, Zbair M, Ait Ahsiane H, Jada A, El Alem N (2020) Microwave assisted green synthesis of Fe_2O_3/biochar for ultrasonic removal of nonsteroidal anti-inflammatory pharmaceuticals. RSC Adv 10(19):11371–11380
69. Ding M, Chen W, Xu H, Shen Z, Lin T, Hu K, Lu C, Xie Z (2020) Novel A-Fe_2O_3/MXene nanocomposite as heterogeneous activator of peroxymonosulfate for the degradation of salicylic acid. J Hazard Mater 382:121064–121073
70. Niu L, Zhang G, Xian G, Ren Z, Wei T, Li Q, Zhang Y, Zou Z (2021) Tetracycline degradation by persulfate activated with magnetic γ-Fe_2O_3/CeO_2 catalyst: performance, activation mechanism and degradation pathway. Sep Purif Technol 259:118156–118167
71. Shan S, Wang W, Liu D, Zhao Z, Shi W, Cui F (2020) Remarkable phosphate removal and recovery from wastewater by magnetically recyclable $La_2O_2CO_3/\gamma$-Fe_2O_3 nanocomposites. J Hazard Mater 397:122597–122609
72. García-Muñoz P, Zussblatt NP, Pliego G, Zazo JA, Fresno F, Chmelka BF, Casas JA (2019) Evaluation of photoassisted treatments for norfloxacin removal in water using mesoporous Fe_2O_3–TiO_2 materials. J Environ Manag 238:243–250
73. Abdel-Wahab AM, Al-Shirbini AS, Mohamed O, Nasr O (2017) Photocatalytic degradation of paracetamol over magnetic flower-like TiO_2/Fe_2O_3 core-shell nanostructures. J Photochem Photobiol A Chem 347:186–198
74. Chahm T, Rodrigues CA (2017) Removal of ibuprofen from aqueous solutions using O-carboxymethyl-N-laurylchitosan/γ-Fe_2O_3. Environ Nanotechnol Monit Manag 7:139–148
75. Lin YP, Mehrvar M (2018) Photocatalytic treatment of an actual confectionery wastewater using $Ag/TiO_2/Fe_2O_3$: optimization of photocatalytic reactions using surface response methodology. Catalysts 8(10):1–17
76. Ding X, Wang S, Shen W, Mu Y, Wang L, Chen H, Zhang L (2017) Fe@Fe_2O_3 promoted electrochemical mineralization of atrazine via a triazinon ring opening mechanism. Water Res 112:9–18
77. He DQ, Luo HW, Huang BC, Qian C, Yu HQ (2016) Enhanced dewatering of excess activated sludge through decomposing its extracellular polymeric substances by a Fe@Fe_2O_3-based composite conditioner. Bioresour Technol 218:526–532
78. Cao Y, Zhou G, Zhou R, Wang C, Chi B, Wang Y, Hua C, Qiu J, Jin Y, Wu S (2020) Green synthesis of reusable multifunctional γ-Fe_2O_3/bentonite modified by doped TiO_2 hollow spherical nanocomposite for removal of BPA. Sci Total Environ 708:134669–134690

79. Pan L, Cao S, Liu R, Chen H, Jiang F, Wang X (2019) Graphitic carbon nitride grown in situ on aldehyde-functionalized α-Fe_2O_3: all-solid-state Z-scheme heterojunction for remarkable improvement of photo-oxidation activity. J Colloid Interf Sci 548:284–292
80. Gao P, Chen X, Hao M, Xiao F, Yang S (2019) Oxygen vacancy enhancing the Fe_2O_3–CeO_2 catalysts in Fenton-like reaction for the sulfamerazine degradation under O_2 atmosphere. Chemosphere 228:521–527
81. Huo Q, Qi X, Li J, Liu G, Ning Y, Zhang X, Zhang B, Fu Y, Liu S (2019) Preparation of a direct Z-scheme A-Fe_2O_3/MIL-101(Cr) hybrid for degradation of carbamazepine under visible light irradiation. Appl Catal B Environ 255:117751–117762
82. Yan P, Shen J, Yuan L, Kang J, Wang B, Zhao S, Chen Z (2019) Catalytic ozonation by Si-doped A-Fe_2O_3 for the removal of nitrobenzene in aqueous solution. Separat Purif Technol 228:115766–115776
83. Gao P, Song Y, Hao M, Zhu A, Yang H, Yang S (2018) An effective and magnetic Fe_2O_3–ZrO_2 catalyst for phenol degradation under neutral pH in the heterogeneous Fenton-like reaction. Separat Purif Technol 201:238–243
84. Wang JC, Li Y, Li H, Cui ZH, Hou Y, Shi W, Jiang K, Qu L, Zhang YP (2019) A novel synthesis of oleophylic Fe_2O_3/polystyrene fibers by Γ-Ray irradiation for the enhanced photocatalysis of 4-chlorophenol and 4-nitrophenol degradation. J Hazard Mater 379:120806–120815
85. Yousif Mohamed Salih F, Sakhile K, Shaik F, Lakkimsetty NR (2020) Treatment of petroleum wastewater using synthesised haematite (α-Fe_2O_3) photocatalyst and optimisation with response surface methodology. Int J Environ Anal Chem 1:1–20
86. Fouda A, Hassan SED, Saied E, Azab MS (2021) An eco-friendly approach to textile and tannery wastewater treatment using maghemite nanoparticles (γ-Fe_2O_3-NPs) fabricated by *Penicillium expansum* strain (K–w). J Environ Chem Eng 9(1):104693–104712
87. Yuan M, Yan F, Chen Y, Luo J, Li Z (2020) A three-dimensional electrochemical oxidation system with α-Fe_2O_3/PAC as the particle electrode for ammonium nitrogen wastewater treatment. RSC Adv 10(15):8773–8779
88. Mei Y, Zeng J, Sun M, Ma J, Komarneni S (2020) A novel Fenton-like system of Fe_2O_3 and $NaHSO_3$ for Orange II degradation. Separat Purif Technol 230:115866–115872
89. Noreen S, Mustafa G, Ibrahim SM, Naz S, Iqbal M, Yaseen M, Javed T, Nisar J (2020) Iron oxide (Fe_2O_3) prepared via green route and adsorption efficiency evaluation for an anionic dye: kinetics, isotherms and thermodynamics studies. J Mater Res Technol 9(3):4206–4217
90. Xu Y, Guo X, Zha F, Tang X, Tian H (2020) Efficient photocatalytic removal of orange II by a Mn_3O_4–FeS_2/Fe_2O_3 heterogeneous catalyst. J Environ Manag 253:109695–109705
91. Davarnejad R, Azizi J (2016) Alcoholic wastewater treatment using electro-Fenton technique modified by Fe_2O_3 nanoparticles. J Environ Chem Eng 4(2):1–8
92. Li J, Guo R, Ma Q, Chao Nengzi L, Cheng X (2019) Efficient removal of organic contaminant via activation of potassium persulfate by γ-Fe_2O_3/α-MnO_2 nanocomposite. Separat Purif Technol 227:115669–115678
93. Luo T, Feng H, Tang L, Lu Y, Tang W, Chen S, Yu J, Xie Q, Ouyang X, Chen Z (2020) Efficient degradation of tetracycline by heterogeneous electro-Fenton process using Cu-doped Fe@Fe_2O_3: mechanism and degradation pathway. Chem Eng J 382:122970–122981
94. Salman HM, Mohammed AA (2019) Extraction of lead ions from aqueous solution by co-stabilization mechanisms of magnetic Fe2O3 particles and nonionic surfactants in emulsion liquid membrane. Colloids Surf A Physicochem Eng Aspects 568:301–310